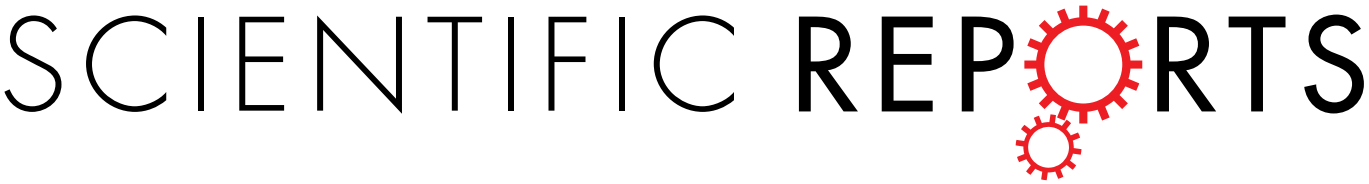

OPEN

Fractal features of soil particle size distributions and their potential as an indicator of *Robinia pseudoacacia* invasion[1]

Received: 7 July 2017
Accepted: 5 April 2018
Published online: 04 May 2018

Kun Li[1], Huanxiang Yang[1], Xu Han[1], Lingyu Xue[1], Yang Lv[1], Jinhua Li[1], Zhanyong Fu[1], Chuanrong Li[1], Weixing Shen[2], Huiling Guo[2] & Yikun Zhang[2]

To study the fractal dimensions of the soil particle size distributions (PSDs) within different plantations (of *Pinus densiflora*, *Quercus acutissima*, *Robinia pseudoacacia*, and *Larix kaempferi*) and evaluate PSDs as an indicator of the likelihood of *Robinia pseudoacacia* invasion, the soil porosity of 0–20 cm soil layers was measured at different plantations in the Yaoxiang Forest Farm, Shandong Province, China. The results showed that the fractal dimension (D_m) values varied from 2.59 to 2.70 among the different plantations and were significantly negatively correlated to sand content and positively correlated to silt content and clay content. Significant negative correlations were observed between D_m and both soil organic matter (SOM) ($P < 0.05$) and available phosphorus ($P < 0.01$). The multifractal entropy dimension (D_1) and entropy dimension/capacity dimension (D_1/D_0) parameters were not significantly correlated with SOM, although significant correlations were found between SOM and each of D_0, $\Delta\alpha$, and $\Delta f(\alpha)$. Compared with the other plantations, the *Robinia pseudoacacia* plantation had higher nutrient contents, higher D_0 and D_1 values and lower D_m values. Based on principal component analysis (PCA) ordination, we concluded that *Robinia pseudoacacia* and *Pinus densiflora* shared a similar habitat and that *Robinia pseudoacacia* is more likely to invade *Pinus densiflora* plantations for soil.

Soil is a porous medium with different particle compositions that display irregular shapes and self-similar structures, and it exhibits fractal characteristics. Therefore, fractal theory has been applied to the study of soil characteristics[1]. Texture is determined by the distribution of different particle size fractions and represents a fundamental characteristic of soil that has a profound influence on physical, chemical and biological processes[2]. The distribution equation of the particle weight/size distribution has been calculated as the fractal dimension of the soil particle size distribution, which can be used to characterize the size and uniformity of soil[3] and can serve as a useful parameter for monitoring soil degradation induced by land-use patterns and changes[4]. Furthermore, the fractal dimension is a measure of the fragility of the fragmented material[5]. The mass fractal dimension of soil particles is one of the inherent properties of soil, and certain assumptions, such as uniform density, which have been questioned when calculating the soil-mass fractal dimension[6]. Therefore, the concept of the volume fractal dimension was developed, and a formula to calculate the soil volume fractal dimension was introduced[7]. The volume fractal dimension of soil particles is a fundamental characteristic of soil. Presently, research on soil particle size distributions (PSDs) is primarily focused on a single dimension[8,9], and this topic has been well studied[10–12]. However, many studies with detailed experimental data have shown that a single fractal dimension is not sufficient to describe PSDs in soil[13]. To obtain more detailed information on soil PSDs, multifractal techniques have been adopted from information science into soil science[14].

Multifractal and fractal geometry usually serve quantitatively as a measure for the internal structural disorder and irregularity[15], which connects back to the basis (Rényi Entropy) on which it is defined[16]. As a result, in addition to geometric objects, the multifractal analysis is also applied to topological and stochastic objects as well and unveils an underlying geometric links to their complexity through an information-theoretic measure[17], identify

[1]Taishan Forest Ecosystem Research Station/Shandong Provincial Key Laboratory of Soil Erosion and Ecological Restoration, Taian, Shandong, 271018, China. [2]Taishan Scenery and Scenic Spot Area Management Committee, Taian, Shandong, 271000, China. Correspondence and requests for materials should be addressed to C.L. (email: chrli@sdau.edu.cn)

geochemical anomalies[18] and decompose and analyze the particulate matter concentrations[19]. Multifractal analysis is suitable for variables with self-similar distributions on a spatial domain, which can provide insight into the spatial variability of soil parameters[20], and several multifractal parameters and two spectra have been proposed by pedologists[21]. Multifractal techniques are promising alternatives to single fractal dimensions because they show well-defined scaling properties, and detailed information can be obtained from a distribution[22,23]. Fractal and multifractal soil parameters can provide potential indicators of soil quality influenced by land use and are capable of characterizing spatial and temporal differences in different land-use patterns[24,25]. These parameters have been applied to soil erosion[26], layered sediments[27] and changes in the carbon and nitrogen distributions in soil[9,28]; however, only a few studies have applied the fractal dimension (D_m) to soil PSDs during a biological invasion.

Soil organic matter (SOM) and nitrogen are important components of soil quality and are widely used in soil quality evaluations[29]. SOM plays unique roles in the maintenance and recovery of soil functions, physical integrity, fertility and environmental quality[30]. In addition, soil quality can affect the structure of vegetation, the growth of plants and litter decomposition and return, which can lead to further impacts on SOM[31] and nitrogen contents[32]. Decreases in nitrogen content can reduce soil fertility, nutrient supplies, porosity, and permeability[33]. In contrast, the succession of vegetation causes changes in soil properties, such as in SOM and nitrogen contents[32]. Different nutrients are needed for the normal growth of plant species, and changes in soil properties will lead to changes in the forest community[34]. The original species might be replaced by species more suited to the soil properties[35]. Therefore, when an invasion occurs, it changes the soil environment in the habitat, weakens the coordination between local species and the soil, and results in succession. Many studies have shown that SOM and nitrogen are significantly correlated with the fractal dimension of soil particle size[24,36], with fine soil particles capable of retaining more organic carbon[37]. Therefore, studying the relationships between soil particle size and soil nutrients is helpful for developing a better understanding of soil characteristics.

Robinia pseudoacacia is a pioneer tree species native to North America, and it grows under a wide range of climate conditions[38]. This tree has been successfully cropped for biomass production and planted in post-mining areas characterized by water limitation and harsh edaphic conditions. Because this species reproduces quickly and is able to live in symbiosis with rhizobia and thus fix atmospheric nitrogen, it has potential as a key species for short-rotation plantations on marginal land. *Robinia pseudoacacia* can significantly improve the conservation of water and soil[39], improve the physical structure of soil[40], increase the anti-erosion properties of soil[41], and enhance the nitrogen mineralization rates of soil[42]. *Robinia pseudoacacia* has expanded its range throughout North America and now occurs in all contiguous states and throughout southern Canada. This species is officially listed as invasive in Connecticut and Massachusetts and has been described as invasive in other states[43,44]. *Robinia pseudoacacia* is colonized by arbuscular mycorrhizal fungi (AMF), ectomycorrhizal fungi, and soil-borne pathogens[45], which improve the plant's ability to regenerate root shoots and disperse[46–48]. Thus, it is now invasive in many parts of the world. At the beginning of 17th century, Hungary introduced *Robinia pseudoacacia*, which is now found over 20% of the country, with approximately 2/3 originating from the regeneration of root shoots. Subsequently, the development of coppice production and the ecological functions of the ecosystems in which it occurs have declined dramatically. In China, *Robinia pseudoacacia* was introduced to Tai'an in the 1920s and gradually became the main tree species of the Taishan Mountain vegetation below 1000 m altitude, where it has seriously restricted the growth of native tree species and led to environmental deterioration. Studies have shown that root regeneration is the mode of population dispersal in *Robinia pseudoacacia*, and under increased interference, it produces a greater number of suckers; thus, its dispersal ability is directly and positively related to soil nutrients[49]. We expect to observe relationships among soil nutrients, PSDs and *Robinia pseudoacacia* invasion; therefore, in this study, we evaluate the ability of this species to invade different habitats based on soil properties to inform our theory of *Robinia pseudoacacia* invasion.

Ordination methods, which are considered robust quantitative analysis techniques, are used to analyze entities as well as their attributes and correlations with environmental variables[50,51]. However, these methods have rarely been used to study PSDs. Gui[52] was the first to analyze the variations in the characteristics of PSDs and the relationships between PSDs and environmental factors by ordination. Gui indicated that ordination methods could be useful for PSD research and suggested that the combination of fractal measurements and ordination methods could provide comprehensive information on PSDs. When the habitat of native plant communities is similar to the habitat of invasive species, the possibility of invasion occurs[53]. Thus, in this paper, we use fractal-scaling theory to analyze the soil properties of four plantations, the preferred environment of *Robinia pseudoacacia* and the similarities among the four plantation soil environments using ordination methods, which can improve our evaluative indicators of habitat invasibility. The objectives of this study were to 1) assess the effects of forests on soil physical properties and 2) explore the potential of the fractal dimension of soil PSDs as an integrating index for quantifying habitat similarity, thereby providing a theoretical basis for revealing the diffusion mechanism of *Robinia pseudoacacia*.

Results

Soil fractal characteristics of the different plantations. The soil size particle composition was measured using a laser particle-size analyzer. The cumulative frequency curves of the soil PSDs in the four plantations are shown in Fig. 1. The figure shows that when the cumulative distribution frequency of the soil particle size reached 50%, the particle size of the *Robinia pseudoacacia* (RP) plantation was 0.02–71 μm, the particle size of the *Pinus densiflora* (PD) plantation was 0.02–40 μm, the particle size of the *Quercus acutissima* (QA) plantation was 0.02–35 μm, and the particle size of the *Larix kaempferi* (LK) plantation was 0.02–20 μm. At PSDs of 0.02–200 μm, the cumulative distribution frequencies of the soil particle sizes of the RP, PD, QA, and LK plantations were 72.47%, 75.90%, 80.27%, and 88.54%, respectively.

The soil PSDs and D_m values of the sampling sites are shown in Table 1. The PSDs vary considerably among the four plantations. The predominant soil particle size categories are silt and sand, with percentages ranging between

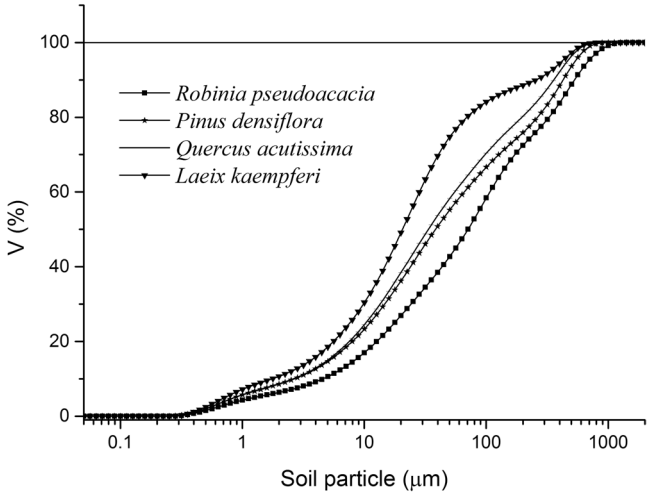

Figure 1. Frequency distribution of volume accumulation content of the soil particles in different plantations.

Plantations	Clay (%)	Silt (%)	Sand (%)	D_m	R^2
Robinia pseudoacacia	5.47 ± 1.58c	32.01 ± 10.84c	62.52 ± 12.33a	2.59 ± 0.05b	0.9402
Pinus densiflora	8.08 ± 1.89b	44.96 ± 7.52b	46.96 ± 8.81b	2.65 ± 0.04a	0.8952
Quercus acutissima	8.22 ± 0.26b	47.81 ± 7.40b	43.98 ± 7.52b	2.66 ± 0.01a	0.8796
Larix kaempferi	10.09 ± 1.58a	62.24 ± 2.27a	27.67 ± 3.12c	2.70 ± 0.01a	0.8080

Table 1. Compositions of the soil PSDs and D_m values in different plantations. Notes: Values are the means of three replications ± SD. Means within a column followed by different letters are significantly different ($P < 0.05$). An R^2 value below 0.95 is acceptable.

32.01% and 62.24% and 27.67% and 62.52%, respectively. The content of clay is relatively low, at only 5.47–10.09%. For clay, silt and sand, the plantations rank LK > QA > PD > RP, LK > QA > PD > RP, and RP > PD > QA > LK, respectively. These results indicate that for the RP plantation, the content of sand is high, and the contents of clay and silt are low. The QA and PD plantations are similar, whereas the LK plantation presents a different pattern. These results indicate that the RP plants might prefer an environment with a high proportion of sand and thus prefer the soil environments of the PD and QA plantations. Linear regression analyses were performed to determine the strength of the relationships between D_m and the clay, silt and sand contents in the 0–20 cm soil layer (Fig. 2). The results show that the fractal dimensions of the PSDs were strongly positively correlated with the clay and silt contents (Fig. 2A,C; $R^2 = 0.9554$ and 0.8255, respectively) and negatively correlated with the sand content (Fig. 2B; $R^2 = 0.8665$). Soils with higher silt-clay contents and lower sand contents had higher D_m values.

The D_m values of the soil PSDs for the four plantations were determined using Eq. (1) and the determination coefficients (R^2 values) in Table 2. The R^2 values range between 0.808 (LK) and 0.9402 (RP), and these values are very similar to the experimental data of Liu[8]. These results indicate that for the different plantations, using the power law or single fractal dimension as a descriptor for soils within these PSDs provides sufficient accuracy. The D_m values range from 2.59 (RP) to 2.70 (LK) and are significant at the 0.05 confidence level, which indicates that the plantations show obvious fluctuations in fractal features. The D_m values are ordered LK > QA > PD > RP, and significant differences were observed in the D_m values between the RP plantation and the other plantations. The fractal dimensions of the RP soil were much lower than those of the other three soils. These changes are consistent with those of clay and silt and inconsistent with those of sand, which indicates that the particle size characteristics of the RP plantation are similar to those of the PD plantation.

Soil multifractal characteristics of the different plantations. Based on Eqs (3–6), the Rényi dimension spectra $D_{(q)}$ of the different plantations were calculated for $-10 \le q \le 10$ at 0.5 lag increments; they are shown along with their standard error bars in Fig. 3. The calculated $D_{(q)}$ values indicated that the reported properties are closer to the singular measure spectra than they are to the soft density spectra. This observation suggests that multifractal models can accurately simulate the internal structure of the constructed measures from soil PSDs. This assumption was tested[54,55] in simulations of the soil PSDs via Iterated Function Systems, and the results indicated the suitability of multifractal measures for modeling these distributions.

As shown in Fig. 3, Rényi spectra of the soil PSDs of *Pinus densiflora*, *Quercus acutissima*, *Robinia pseudoacacia*, and *Larix kaempferi* followed a typical anti-S-decreasing function. When $q > 0$, the decreasing trend of $D_{(q)}$ slowed, and the dimensions of the different soils approached 0.9. The $D_{(q)}$ values of *Larix kaempferi* plantation soil changed obviously in the range $-10 \le q \le 10$, which was more inhomogeneous than that of the other soil types. In addition, the *Quercus acutissima* plantation soil was more evenly distributed.

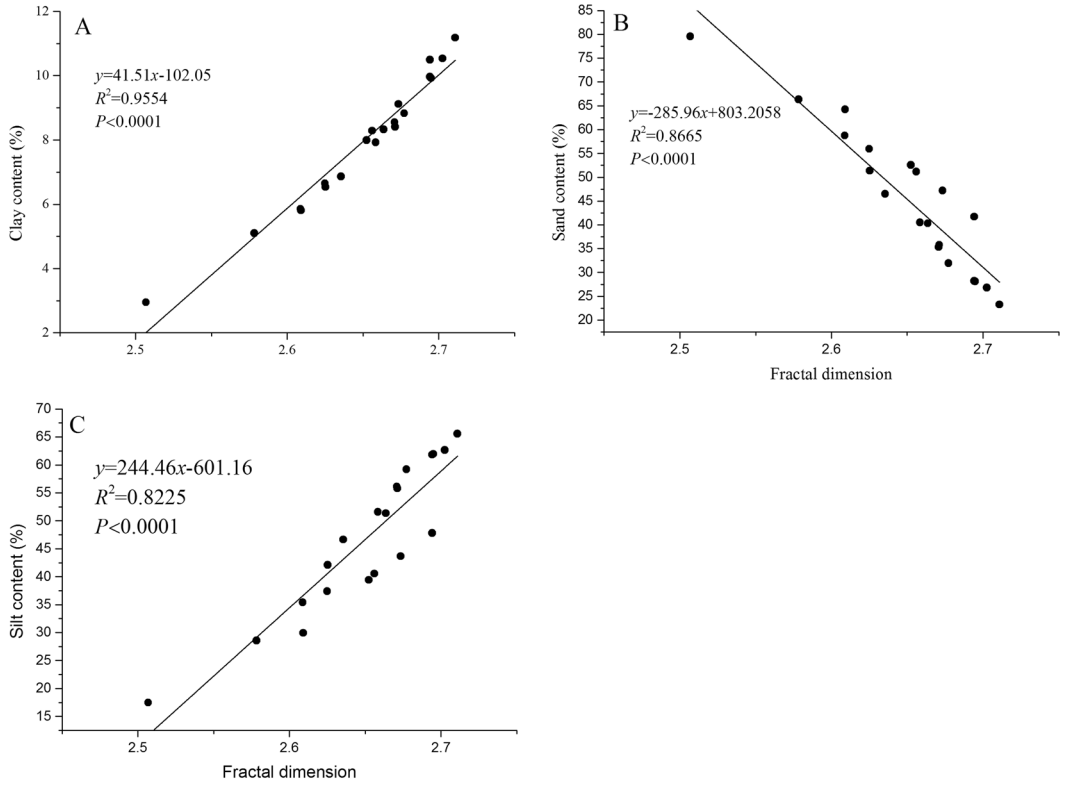

Figure 2. Relationships between soil fractal dimension and (**A**) clay, (**B**) sand, and (**C**) silt content in the 0–20 cm soil layer (n = 20).

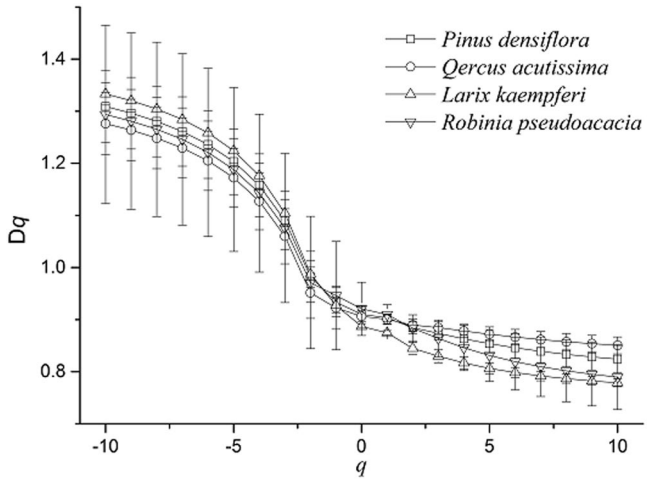

Figure 3. Spectrum curves $D_{(q)}$-q of generalized dimensions in different plantations.

Plantations	D_0	D_1	D_1/D_0	$Hq(q=2)$	$\Delta\alpha$	$\Delta f(\alpha)$
Robinia pseudoacacia	0.921 ± 0.051	0.910 ± 0.019a	0.990 ± 0.044	0.942 ± 0.026	0.953 ± 0.069a	0.943 ± 0.012
Pinus densiflora	0.910 ± 0.014	0.903 ± 0.007a	0.988 ± 0.016	0.942 ± 0.004	0.382 ± 0.019c	0.927 ± 0.006
Quercus acutissima	0.913 ± 0.017	0.901 ± 0.010a	0.994 ± 0.020	0.945 ± 0.003	0.459 ± 0.020c	0.916 ± 0.037
Larix kaempferi	0.887 ± 0.006	0.875 ± 0.004b	0.986 ± 0.009	0.922 ± 0.004	0.760 ± 0.089b	0.934 ± 0.016b

Table 2. Parameters of multifractal spectra of soil particle-size distribution in different plantations. Notes: Values are the means of three replications ± SD. Means within a column followed by different letters are significantly different ($P < 0.05$).

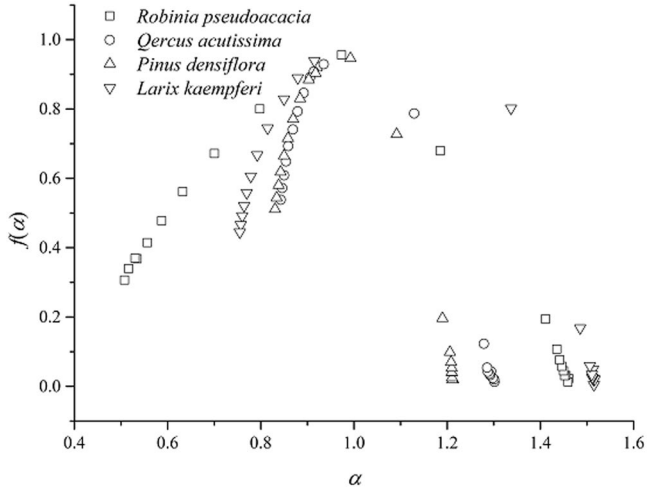

Figure 4. Multifractal spectra ($f(\alpha)$ versus α) for *Robinia pseudoacacia, Pinus densiflora, Quercus acutissima* and *Larix kaempferi*.

Plantation	Regression equation	R^2	*P* value
Robinia pseudoacacia	$Dq = 0.9736Hq - 0.0084$	0.974	0.03557
Pinus densiflora	$Dq = 0.9442Hq + 0.0336$	0.9649	0.03119
Quercus acutissima	$Dq = 0.9768\mathrm{Hq} + 0.0154$	0.9768	0.02954
Larix kaempferi	$Dq = 0.9753Hq - 0.0041$	0.9803	0.02761
Total	$Dq = 0.9643Hq - 0.0084$	0.9739	0.03071

Table 3. Relationship between the generalized Hurst exponent (Hq) and the generalized fractal dimension (Dq).

The multifractal spectrum provides information about the relative importance of various fractal exponents present in the series. In particular, the width of the spectrum indicates the range of present exponents[56]. Multifractal spectra from different plantations are shown in Fig. 4. Soil particle size distribution $f(\alpha)$ versus α functions were continuous convex functions, indicating that the soil particle distributions from different plantations had heterogeneous properties. This result also indicated that the soil was a complex fractal. The width and shape of a multifractal spectrum can be used to characterize and quantify the properties. A summary of Hurst index values is provided in Table 2, where the range and average of the values characterize the different scenarios contemplated in this work. Here, we focus on the quantification of multifractal spectra amplitudes and symmetries through the difference of the extreme singularities ($\Delta\alpha = \alpha_{max} - \alpha_{min}$) and the difference of their respective $f(\alpha)$ values $\Delta f(\alpha) = f(\alpha_{max}) - f(\alpha_{min})$[20]. In this way, a higher $\Delta\alpha$ value indicates higher complexity of the structure studied in the four plantations. All the spectra in Fig. 4 are strongly asymmetric, with the range on the left side of the plot being much smaller than the range on the right side. The $\Delta\alpha$ value of RP was significantly higher than those of the other plantations, although the $\Delta\alpha$ values of the PD and QA plantations did not change significantly. These results indicated that the heterogeneity of soil particle composition was higher in the RP plantation. A higher $\Delta f(\alpha)$ value indicates higher asymmetry in the multifractal spectra (right-handed if $\Delta f(\alpha) > 0$). The results indicate that the four plantations have high asymmetry.

A one-way ANOVA was performed to assess the differences between the treatments for various parameters derived from the plots of the singularity spectrum; $\Delta\alpha$; $\Delta f(\alpha)$; and the generalized spectrum dimensions, D_0, D_1 and D_1/D_0. The capacity dimension (D_0) was calculated using the box-counting technique. Table 2 shows that the highest D_0 value was observed for the RP plantation (0.921) soil PSDs, whereas lower D_0 values were observed for the LK plantation soil PSDs (0.887). D_0 provides general information about the PSDs system because it represents the dimension of the set of sizes with a non-zero relative volume. $D_0 = 1$ means that all subintervals are occupied at all scales, whereas $D_0 = 0$ means that all subintervals are empty[15]. Therefore, the soil PSDs from the RP plantation occurred over a relatively wide range, whereas the PSDs from the LK plantation presented a relatively low range, and no differences among D_0 values were observed.

Considering that the D_0 values reflect the range of a continuous distribution and that the D_1 values express the range of PSDs and measure the homogeneity among fractions at different partition levels, D_1/D_0 was used to describe the heterogeneity in a distribution as suggested by Posadas[14]. As shown in Table 3, the D_1/D_0 values were ordered QA > RP > PD > LK. $D_1/D_0 = 1$ means that all fractions have equal values at different scales, thus indicating the most heterogeneous distribution. Low D_1/D_0 values reflect a distribution in which irregularities are concentrated.

The D_1/D_0 values of the four plantations ranged from 0.986 to 0.994, which indicated a heterogeneous distribution.

Plantation	AN (mg/kg)	AP (mg/kg)	SOM (g/kg)
Robinia pseudoacacia	115.92 ± 24.86a	37.76 ± 9.75a	21.4 ± 4.37a
Pinus densiflora	86.13 ± 9.69b	18.13 ± 4b	13.56 ± 2.28b
Quercus acutissima	63.73 ± 13.37b	13.37 ± 6.8b	9.32 ± 2.02c
Larix kaempferi	83.89 ± 4.31c	11.29 ± 2.08b	11.42 ± 2.39bc

Table 4. SOM, AN and AP contents in the 0–20 cm layer at each plantation. Notes: Values are the means of three replications ± SD. Means within a column followed by different letters are significantly different ($P < 0.05$).

	Clay (%)	Silt (%)	Sand (%)	D_m	D_1/D_0	D_0	D_1	$\Delta f(\alpha)$	$\Delta\alpha$
AN	−0.447*	−0.407	0.418	−0.418	0.202	0.432	0.407	0.258	0.575**
AP	−0.734**	−0.611**	0.636**	−0.731**	0.073	0.507*	0.375	0.29	0.547*
SOM	−0.557*L	−0.535*	0.545*	−0.545*	0.013	0.568*	0.386	0.452*	0.551*

Table 5. Relationships between soil chemical properties and soil physical properties. *Pearson correlation is significant at $P < 0.05$; **Pearson correlation is significant at $P < 0.01$.

The values of the entropy dimension (D_1) were ranked RP > PD > QA > LK. D_1 provides a measure of the heterogeneity of PSDs[17]. When the D_1 value is higher, the soil's PSDs are more heterogeneous, the PSD range is wider, and the measures are more homogeneous among regions over all sets. Significant differences in D_1 values were detected among the four plantations at the 95% confidence level. The D_1 values of the soil PSDs from the LK plantation were significantly lower than those of the other three plantations. The $\Delta\alpha$ values of the RP plantation were significantly higher than those of the other plantations, and there were no significant relationships among the four plantations.

At different time scales, the Hurst exponent was greater than 0.5, which indicated that the time series of the four plantations are non-random. persistent, and take on long-range dependence; in general, the time series of particle size distribution showed an upward or downward trend. Thus, in the future, it will improve. In all cases, we found a linear relationship between Hq and Dq. The R^2 values were consistently higher than 0.96 at $P < 0.05$ (see Table 3). The P value of the relationship for the LK plantation was lowest, and the R^2 value was highest for this plantation. Overall, the generalized Hurst exponent was linearly related to the generalized fractal dimension ($R^2 = 0.9739$, $P = 0.03071$).

Relationships between multifractal parameters and soil properties. SOM, available nitrogen (AN) and available phosphorus (AP) were selected as the soil quality indicators. Table 4 shows that the contents of SOM, AN and AP in the RP plantation were higher than those in the other three plantations (21.40 g/kg, 115.92 mg/kg and 37.76 mg/kg, respectively) and the differences were significant at the 0.05 level. These results indicate that planting RP can improve soil quality and show that the dispersal of RP is strongly correlated with SOM and AN[42]. The SOM and AN values were ordered as follows: RP > PD > LK > QA.

A simple correlation analysis was performed to establish the relationships between D_m and the sand, silt, and sand contents. The results indicate that the fractal dimension of the PSDs was highly significantly and positively correlated with the contents of clay and silt ($R^2 = 0.9554$ and 0.8255, respectively) and negatively correlated with the content of sand ($R^2 = 0.8665$), which indicates that the removal of fine particles (clay and silt particles) results in decreased D_m values. The decrease in D_m indicates a decrease in fine particles and their accumulation in coarser fractions.

To analyze the relationships between the different parameters, a simple correlation analysis was conducted and the correlation between multifractal parameters and soil properties are shown in Table 5. The multifractal parameters were consistent in reflecting the multifractal law of soil particle composition. Among the soil properties, SOM was positively and significantly correlated with AN, AP, $\Delta f(\alpha)$ and $\Delta\alpha$, which are indices of soil quality that reflect the soil nutrient conditions. Here, SOM was significantly positively correlated with D_0, whereas it showed a weak or no correlation with D_1/D_0 and D_1. The highest correlation coefficient was observed for SOM and D_0. In addition, SOM increased as D_m decreased.

Habitat similarity analysis. A direct gradient analysis was used to describe the soil habitat similarity based on changes in the habitat. The four plantations were classified using Canoco 5.0, and detailed information was obtained on the clay, silt, and sand contents; D_m; AN; AP; SOM; D_1/D_0; D_0; D_1; $\Delta f(\alpha)$ and $\Delta\alpha$. The plantation distribution patterns were analyzed by PCA. The eigenvalues of the four PCA axes were 0.7130, 0.1450, 0.0823 and 0.0285. Figure 5 shows the PCA ordination diagram based on the first and second axes. In Fig. 5, the values for each plantation occur within a limited range and are clearly separated from those of the other plantations. The RP plantation was similar to the PD plantation and dissimilar to the LK plantation, and cross-correlations were observed among the PD, QA and LK plantations. These results indicate that the RP and PD trees share similar habitats.

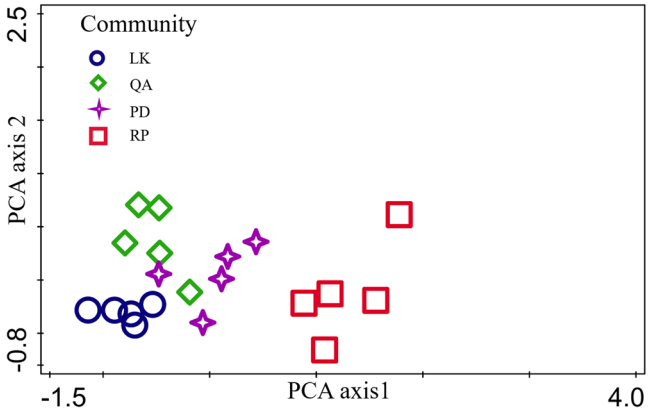

Figure 5. Two-dimensional PCA ordination diagram of plantation soil properties.

Discussion

Soil PSDs are commonly used to classify soils and estimate various related soil properties[57]. Fractal geometry has been increasingly applied as an effective tool for describing the structure, dynamics, and physical processes of soil, thereby facilitating a better understanding of the performance of a soil system[1,8]. Therefore, in this paper, we studied the fractal characteristics of soil in different plantations. Our analyses revealed significant positive correlations between D_m and clay and silt contents ($R^2 = 0.9554$ and $R^2 = 0.8255$, respectively) and a significant negative correlation between D_m and sand content ($R^2 = 0.8665$). These results indicate that the soil clay content affects the D_m value, which is also affected by the maximum size of the soil particles. These findings are similar to those of other studies[8,9,27,58,59]. The results indicate that smaller particle sizes reflect a greater spatial filling capacity of the soil, which corresponds to higher fractal dimension values based on pore geometry[13]. In addition, we found that the sand content of the RP plantation was significantly higher than the sand contents of the QA, PD and LK plantations ($P < 0.05$), whereas the clay and silt contents showed the opposite trend ($P < 0.05$). These results indicate that the RP plantation achieved a lower D_m value due to a higher sand content. Thus, RP might prefer soil environments with higher sand contents and might invade habitats with such contents more easily than can other plants.

The fractal dimension is a sensitive and useful index for quantifying changes in the properties of soil[60], and several linear relationships have been observed between fractal dimensions and soil properties[61]. The proportion of each fraction has a dominant influence on many soil properties. The clay fraction constitutes the reactive fraction of the soil, whereas the sand and silt fractions are relatively inert[62] and can partially reflect the stability of a plant community[59]. Therefore, the relationships between D_m and soil physical-chemical properties were studied here. The results show that soil PSDs can influence the soil water infiltration and moisture retention and the availabilities of water and nutrients to plants[63], and many model simulations of SOM decomposition and formation have shown that soil PSDs can also control the SOM dynamics[64]. When the fractal dimension is higher, the clay content is higher, and a larger surface area, a stronger bond, and more nutrients are observed[65]; these factors significantly improve the SOM[9]. In addition, higher SOM is beneficial for the retention of fine soil particles[26,37,66], whereas D_m is negatively correlated with SOM[59]. Our results indicated significant and negative correlations between D_m and each of the clay and silt contents, SOM and AP, whereas significant and positive correlations were observed among sand content, SOM and AP. The fractal dimension of soil PSDs can quantify the properties of soil particle composition, which reflects the size of soil particles and the relationship between particle size and the degree of soil thickness. The fractal dimension of soil texture can be characterized from sand to fine changes. This finding may reflect correlations between the PSDs and the microbial community composition[67,68] and may demonstrate the responses of plant and forest communities to soil heterogeneity[69]. The latter is a basic element for competitive and facilitative interactions between plants[70] and can determine the patterns of plant and community distributions[71]. The root structures of various plant species might be a source of differences in the fractal dimension[72]. The RP plantation at Mountain Tai presents a stronger diffusivity and a developed root system that shows increases in residual inputs and the concentrations of fine roots with abandonment age[73,74]. Additionally, these plantations release large amounts of soil nutrients[75], which improves the soil nutrient conditions. Although the LK plantation had the highest D_m value, this value was correlated with the content of allelochemicals in the root exudates, and lower nutrient allelochemicals contribute greatly to the cohesion of fine soil particles[60]. D_m reflects the spatial filling capacity of soil based on the distribution of soil particles[33,76], although reductions of SOM and TN levels will result in decreased soil fertility, soil nutrient supplies, soil porosity, soil penetrability and soil productivity[77]. Then, D_m is improved[3].

The heterogeneity of multifractal spectra can be assessed in different ways[78]. For example, the curvature and symmetry of the $f(\alpha)$ spectra provide information on the heterogeneity, which can also be assessed by the magnitude of changes around D_0 in both $f(\alpha)$ and α[14]. The width of the $f(\alpha)$ spectrum is defined as the difference between the most positive and negative moments used in the evaluation of the singular spectra and the moment order zero ($\Delta\alpha$). This width may be considered as an indicator of symmetry/asymmetry of a multifractal system[79]. For the independent random process, with no correlation among samples, $H_q = 0.5$. The observational time series is persistent for $H_q > 0.5$, whereas the sequence shows anti-persistent behavior for $H_q < 0.5$[80]. The H_q

Species	Cover/%	Frequency/%	Density/plants/hm^2
Diospyros lotus	25	30	5000
Robinia pseudoacacia	10	17	2660
Broussonetia kurzii	20	3.3	670
Pistacia chinensis	5	7	670
Quercus acutissima	5	3.3	670

Table 6. Regeneration of tree species in the *Pinus densiflora* planation.

values of the four plantations were higher than 0.5, indicating they are persistent. The generalized dimension, D_q, is a constant in the case of scale invariant distributions but changes with q for multifractal measures. A D_1 value close to D_0 should be an indication of a measure distributed over all the study scales, whereas a D_1 value close to 0 should reflect irregularities, indicating that most of the measure is concentrated within a small size domain of the study scale. The ratio D_1/D_0 may be considered a measure of evenness in the context of multifractal spectra[23]. Thus, low values of this parameter reflect a distribution in which irregularities are concentrated, whereas high values indicate the opposite. D_0, D_1, and D_1/D_0 may be seen as indicators of abundance, dispersion and evenness, respectively[62]. The D_0 values of the RP, PD, QA, and LK plantations were 0.921, 0.910, 0.913, and 0.887; these values indicate four degrees of abundance, which in this case alludes to the scaling of the number of cells containing some particle volume and further suggest similitude of the studied PSDs. The capacity dimension, D_0, ranged from 0.887 to 0.921, the entropy dimension, D_1, ranged from 0.875 to 0.910, and the ratio D_1/D_0 ranged from 0.986 to 0.994. These values indicate somewhat diverse scaling properties among the soil samples, and the ranges of values suggest that none of these single parameters should be used to discriminate among measures, specifically PSDs in our case study.

The multifractal parameters were significantly correlated with SOM[81]. Therefore, in this study, a multifractal analysis of the samples was conducted. As shown above, the D_0, D_1, and D_1/D_0 values reflected different information on the soil PSDs, and plantation type had an influence on the D_0, D_1, and D_1/D_0 values. The fractal dimensions (D_1, D_m) that mainly reflect fine soil particles are highly correlated with the SOM content of soils. The fractal dimension D_0 can provide useful information on the coarse particle fraction[82]. Table 6 shows that significant correlations were not present between SOM and D_1 or D_1/D_0, although a significant correlation was observed between D_0 and SOM. These findings are inconsistent with those of Wang[81] and Sun[83], who found that D_0 was correlated with the coarse particle fraction[82]. Furthermore, in the present study, the coarse content was positively correlated with the SOM (Table 5).

Invasibility is an emergent property of invaded ecosystems and their established species, and it affects only the extinction rates of the invaders and not their immigration rates[84,85]. Recently, studies have focused on the relationships between communities and invasibility[86,87], but the findings are inconsistent[87]. Studies have shown that local environmental conditions can be used to predict plant invasions[88,89], and niche-based modeling can be used to predict the risk of alien plant invasions at a large scale[85,90–92]. When additional resources are available, a community is more vulnerable to invasion[93]; thus, soil nutrients can affect the invasibility of a plant community. This phenomenon likely offers alien plants a dominant advantage in competition with native plants, and it promotes the likelihood of invasion by alien plants[94,95]. Therefore, we evaluated the soil properties of four plantations (Tables 1–3). In previous work, the degree of similarity between a new environment and a native environment was assessed and found to be beneficial for understanding community invasibility[96]. RP plantations are mainly rooted in Mountain Tai and show strong correlations with the characteristics of the soil; therefore, we can evaluate the community invasibility based on the soil properties. The ordination method can be applied to analyze the variation characteristics of PSDs and the relationships between PSDs and environmental factors[45]. Community invasibility can be used to evaluate the degree of invasion of a region or community. We found that the characteristics of the RP plantations were strongly correlated with those of the PD plantations (Fig. 5), which indicates that RP plants are more likely than are other plants to invade PD habitat. We also found that RP had regenerated in the PD plantation (Table 6), which is consistent with the abiotic suitability hypothesis[97].

Conclusions

We studied the fractal dimension of soil PSDs in soils within plantations of different tree species (PD, QA, RP and LK) and evaluated the possible factors that indicate invasion. The fractal and multifractal characteristics of 20 soil PSDs were studied. The results showed that a law relationship could be applied to all the soil PSDs. D_m varied from 2.59 to 2.70 among the different plantations and reached the highest values in the LK plantations. D_m was negatively correlated with sand content and positively correlated with the silt and clay contents. A significant and negative correlation was observed between D_m and both SOM ($P < 0.05$) and AP ($P < 0.01$). These results suggest that D_m can be used to characterize the uniformity of soil texture to a certain extent as well as the soil fertility characteristics. The D_1 and D_1/D_0 values were not significantly correlated with SOM, whereas the D_0, $\Delta\alpha$, and $\Delta f(\alpha)$ were each significantly correlated with SOM.

Our analyses of the PSDs and soil physical-chemical properties of the different plantations in the study area indicated that the PD, QA and LK plantations presented similar habitats. Compared with the other plantations (PD, QA and LK), the RP plantation had more nutrients, higher D_0 and D_1 values, and lower D_m values. The PCA ordination showed that the habitat of the PD plantation is similar to that of the RP plantation, which indicates that in the same environment, RP is more likely than other species to invade a PD habitat.

Plantations	Slope(°)	Aspect	Altitude /m	Tree height/m	DBH/cm	Density/ha	pH	Soil thickness/cm
Robinia pseudoacacia	40	North	720	15.84	23.92	356	4.94	24.50
Pinus densiflora	26	North	703	12.48	22.62	470	4.67	35.33
Quercus acutissima	23	South	730	13.76	20.41	551	5.00	26.08
Larix kaempferi	29	North	718	15.30	18.25	640	4.98	32.00

Table 7. Basic information on the soil sampling sites.

Materials and Methods

Study area. The study was conducted at the Yaoxiang Forest Farm, in Mount Tai, China. The farm is located on the border of the southern suburbs of the cities Ji′nan and Tai′an and north of the main peak of Mount Tai. The geographical coordinates are 117°10′E and 36°17′N, and the study area is 12 kilometers long and 5 kilometers wide from north to south, with a total area of 1210.2 hectares. The region has a warm temperate continental monsoon climate. The annual average temperature is 10.8 °C; the maximum temperature is 34 °C, and the minimum temperature is −24 °C. The average annual precipitation is 900–1000 mm, and the altitude above sea level ranges from 400–956 m. The soil types are typical of mountain brown terrain, and the soil thickness is 15–90 cm. After years of reforestation, the forest farm consists almost entirely of plantations, which were mostly planted in the 1950s, and includes a small amount of shrub forest.

Soil sampling and analysis. The experimental plot was established in a standard sample of *Pinus densiflora* (PD), *Quercus acutissima* (QA), *Robinia pseudoacacia* (RP) and *Larix kaempferi* (LK) plantations at the Taishan Forest Ecosystem Research Station. The sample plots are described in Table 7. The soil samples were collected from the 0–20 cm soil layer in all plots using the five-spot-sampling method, with five replicates of each sample, for a total of 20 samples. After the removal of residual litter, the samples were air dried, passed through a 2-mm screen, and then returned to the lab for analysis. Each sample was divided into two parts, with one part used to analyze the soil particle composition and the other part ground and passed through a 0.25-mm screen and used to determine the contents of SOM and available nutrients.

The soil PSDs were measured via laser diffraction with a Mastersizer 2000 Particle Size Analyzer (Malvern Instruments, Malvern, England), which has a range of 0.02–2000 μm and repeated measurement errors of less than 2%. From each sample, 0.5 g samples were soaked for 36 h in hyperpure water, stirred, and then heated, and the supernatant was subsequently removed. Each sample was dispersed for 30 s using an ultrasonic wave, and the percentage of the soil particle-volume fraction was determined. The results were presented using the US standard for classifying soil particle size: 0–0.002 mm, 0.002–0.05 mm, 0.05–0.1 mm, 0.1–0.25 mm, 0.25–0.5 mm, 0.5–1 mm, and 1–2 mm. Each sample was then described in terms of the percentages of clay (<0.002 mm), silt (0.002–0.05 mm) and sand (0.05–2 mm). The SOM was determined using the potassium dichromate oxidation method, the AN was determined using the Conway method, and the AP was determined using the double acid extraction method. Each sample was analyzed in duplicate, and the mean values were calculated. This work was conducted based on the forestry standards described in the "Observation methodology for long-term forest ecosystem research" of the People's Republic of China.

Soil fractal model theory. Based on the soil texture classification system of the US and the volume fractal dimension formula deduced by Gao[7], the fractal scaling of PSDs was performed as follows. The cumulative number of soil grains (r) greater than a characteristic size (specific measuring scale, R) is set to be N ($r > R$), and the cumulative volume distribution of soil grains (r) smaller than the specific measuring scale, R, is set to be V ($r < R$). Then, the values of N and V will be proportional to R^D and R^{3-D}, respectively. The exponent D can be easily determined based on the relationship between R and N or V. The fractal fragmentation can be quantified based on the relationship between the number and size in a statistically self-similar system:

$$N(X \geq x_i) = kx_i^{-D} \quad (1)$$

where $N(X > x_i)$ is the cumulative number of objects or fragments X greater than the i-th characteristic size x_i, and k is the number of elements at a unit length scale. However, the relationship given by Eq. (1) is not convenient, and errors can be introduced in the calculation. The applicability of Eq. (1) to PSD analysis is also limited because N values are unavailable in conventional PSD data. Thus, an estimation of D for soil PSD is used here, and the derived equation is as follows:

$$\frac{V_{(r<R)}}{V_T} = \left(\frac{R}{\lambda_V}\right)^{3-D} \quad (2)$$

where V is the cumulative volume of particles of size r and less than R; V_T is the total volume; R is the mean particle diameter (mm) of the R size class; λv is the mean diameter of the largest particle; D is the fractal dimension; and $V(r < R)$ is the sum of objects with fragments less than a characteristic size. The mean particle diameter is the arithmetic mean of the upper and lower sieve sizes. Based on the logarithm of both sides of Eq. (2) and the linear regression between $\log(V_{(r<R)}/V_T)$ and $\log(R/\lambda_V)$, the value of 3-D can be determined[20].

Multifractal analysis. Multifractal sets can be characterized based on the Rényi dimensions of the qth moment orders of distribution, $D_{(q)}$, which were defined by Rényi *et al.*[98] and Hentschel *et al.*[99]. Based on the

measurement interval of the laser particle size analyzer ($I = [0.02\,\mu m, 2000\,\mu m]$), the 100 subintervals are $I_i = [\varphi_i, \varphi_i + 1]$, $i = 1, 2, \ldots, 100$; $\sum_{i=1}^{100} vi = 100$, $v_1, v_2, \ldots, v_{100}$; where v_i is the soil particle size volume percentage of I_i, and φ_i is the measured soil particle size from the laser particle size analyzer. According to the standard particle size division methods for the laser particle size analyzer, $\log(\varphi_i + 1/\varphi_i)$ is constant across the measurement interval of $I = [0.02\,\mu m, 2{,}000\,\mu m]$. To meet the requirements of the multifractal method, $\psi_i = \log(\varphi_i/\varphi_1)$ (with $i = 1, 2, \ldots, 100$) was changed. Next, we obtained a new dimensionless interval of $J = [0, 5]$, which has 100 equidistant subintervals, $Ji = [\psi_i, \psi_i + 1]$, $i = 1, 2, \ldots, 100$. In the interval J, 2^k same size subintervals were used (ε), with $\varepsilon = 5 \times 2^{-k}$. Each subinterval contained at least one measured value within a k range of 1 to 6[29].

Multifractal measures can also be characterized by scaling the qth moments of $[P_i]$ distributions[94] expressed in the following form:

$$\mu_i(q, \delta) = \frac{\mu_i(\delta)^q}{\sum_{i=1}^{n(\delta)} \mu_i(\delta)^q} \tag{3}$$

The Rényi dimension D_q is a monotonous decreasing function for all real q values within the interval $[-\infty, +\infty]$. Parameter q acts as a scanning tool that scrutinizes the denser and rarer regions of the measure μ[23,100,101]. For $q \gg 1$, regions with a high degree of concentration are amplified, whereas for $q \ll -1$, regions with a small degree of concentration are amplified.

The generalized fractal dimensions or Rényi dimensions can be calculated as follows:

$$\mathrm{D}(q) = \lim_{\delta \to 0} \frac{1}{q - 1} \times \frac{\lg[\sum_{i=1}^{n(\delta)} \mu_i(\delta)^q]}{\lg \delta} (q \neq 1) \tag{4}$$

$$D_1 = \lim_{\delta \to 0} \frac{\sum_{i=1}^{n(\delta)} \mu_i(\delta) \lg \mu_i(\delta)}{\lg \delta} (q = 1) \tag{5}$$

The singularity strength $\alpha(q)$ and singularity spectrum $f(\alpha)$ are as follows:

$$\alpha(q) = \lim_{\varepsilon \to 0} \frac{\sum_{i=1}^{N(\varepsilon)} \mu_i(q, \varepsilon) \lg \mu_i(\varepsilon)}{\lg \varepsilon} \tag{6}$$

$$f(\alpha(q)) = \lim_{\varepsilon \to 0} \frac{\sum_{i=1}^{N(\varepsilon)} \mu_i(q, \varepsilon) \lg \mu_i(q, \varepsilon)}{\lg \varepsilon} \tag{7}$$

The graph of $f(\alpha)$ versus α is referred to as the multifractal spectrum and typically has a parabolic concave downward shape, with the range of α values increasing with increasing heterogeneity of the measure. A homogenous fractal exhibits a narrow $f(\alpha)$ spectrum. The $f(\alpha)$ spectrum and the generalized dimensions contain the same information, both characterizing an interwoven ensemble of fractals of dimension $f(\alpha_i)$[20].

where $\mu_i(\delta)$ is the volume percentage of every subinterval, δ is the same size subinterval, q is the given parameter, and $D_{(q)}$ is the information entropy. When $q = 0$, $D(q) = D_0$ (D_0 can measure the span of the soil PSDs). When $q = 1$, $D_{(q)} = D_1$ (D_1 provides the irregular degree of soil PSDs). D_1/D_0 can measure the degree of heterogeneity of the soil PSDs[51]. D_2 is mathematically associated with the correlation function and related to the Simpson diversity index. The relationship among D_0, D_1, and D_2 can be defined as follows:

$$D_2 \leqq D_1 \leqq D_0$$

where the equality $D_2 = D_1 = D_0$ occurs only if the fractal is statistically or exactly self-similar and homogeneous[52].

Multifractal Detrended Fluctuation Analysis (MDFA). MDFA is thoroughly described in Kantelhardt[102]. In the basic approach, time series are first sub-divided into smaller segments from which are subtracted a least-squares best-fit polynomial of a chosen order to remove the artifacts created by non-stationarities in the time series. A method similar to the moment is then applied to the resulting detrended series. MDFA is described in detail in Salat[103] and Chamoli[104]. H_q is the generalized Hurst exponent and characterizes the long-/short-range dependence structure in the series[102]. The variation in H_q with q is useful for understanding the different scaling of small and large fluctuations. For multifractal time series, the scaling behavior of the large fluctuations is characterized by the values of H_q for positive q values. The scaling of the small fluctuations is characterized by the values of H_q for negative q values[104].

Principal Component Analysis. Principal component analysis (PCA) is a general unconstrained linear method widely used for vegetation pattern analysis. The soil parameters of each plantation were used for the PCA. The soil parameters included the multifractal parameters, PSDs, D_m and soil properties. The ordination diagram of species and environmental variables derived from the PCA optimally displays the variation of the object composition in connection with the environmental factors. In our analysis, PCA was performed with the four plantations, and the particle-size fractions and AN, AP, SOM contents were included as environmental variables. The plantations were classified using Canoco 5.0 software, and their distribution patterns in the study area were analyzed by PCA.

Data analysis. A one-way ANOVA was performed to evaluate the effects of plantation on the soil fractal and multifractal parameters, soil AN, soil AP and SOM. The Duncan procedure was used to separate the means of these variables at the $P < 0.05$ level. A correlation analysis was performed to determine the relationships between the multifractal parameters and the quantitative environmental variables using SAS. In this paper, we introduce the method of community ordination to evaluate the similarity of the four plantations based on the soil properties, and the distribution patterns of soil properties in the study area were analyzed via a PCA, which is a general unconstrained ordination method for vegetation pattern analysis, using Canoco 5.0.

References

1. Perfect, E. & Kay, B. D. Fractal theory applied to soil aggregation. *Soil Sci Soc Am J.* **55**(6), 1552–1558 (1991).
2. Tyler, S. W. & Wheatcraft, S. W. Fractal scaling of soil particle-size distributions: analysis and limitations. *Soil Sci Soc Am J.* **56**(2), 362–369 (1992).
3. Yang, P. L., Luo, Y. P. & Shi, Y. C. Fractal features of soil characterized by particle weight distribution. *Chin Sci Bull.* **38**(20), 1–896 (1993).
4. Wang, X., Li, M. H., Liu, S. & Liu, G. Fractal characteristics of soils under different land-use patterns in the arid and semiarid regions of the Tibetan Plateau, China. *Geoderma.* **134**(1), 56–61 (2006).
5. Turcotte, D. L. Fractals and fragmentation. *J. Geo Res Solid Earth* **91**(B2), 1921–1926 (1986).
6. Martí, M. Á. Laser diffraction and multifractal analysis for the characterization of dry soil volume-size distributions. *Soil Till Res.* **64**(1), 113–123 (2002).
7. Gao, G. L. *et al*. Fractal scaling of particle size distribution and relationships with topsoil properties affected by biological soil crusts. *PloS One* **9**(2), e88559 (2014).
8. Liu, X., Zhang, G., Heathman, G. C., Wang, Y. & Huang, C. H. Fractal features of soil particle-size distribution as affected by forest communities in the forested region of mountain Yimeng, China. *Geoderma.* **154**(1–2), 123–130 (2009).
9. Xu, G., Li, Z. & Li, P. Fractal features of soil particle-size distribution and total soil nitrogen distribution in a typical watershed in the source area of the middle Dan river, China. *Catena.* **101**(2), 17–23 (2013).
10. Jin, Z., Dong, Y. S., Qi, Y. C., Liu, W. G. & An, Z. S. Characterizing variations in soil particle-size distribution along a grass-desert shrub transition in the Ordos plateau of Inner Mongolia, China. *Land Degrad Dev.* **24**(2), 141–146 (2013).
11. Doublet, J. *et al*. Distribution of c and n mineralization of a sludge compost within particle-size fractions. *Bioresource Technol.* **101**(4), 1254–1262 (2010).
12. Keller, T. & Håkansson, I. Estimation of reference bulk density from soil particle-size distribution and soil organic matter content. *Geoderma.* **154**(3–4), 398–406 (2010).
13. Millan, H., Gonzalez-Posada, M., Aguilar, M., Domınguez, J. & Céspedes, L. On the fractal scaling of soil data. *Particle-size distributions. Geoderma.* **117**(1), 117–128 (2003).
14. Posadas, A. N., Giménez, D., Bittelli, M., Vaz, C. M. & Flury, M. Multifractal characterization of soil particle-size distributions. *Soil Sci Soc Am J.* **65**(5), 1361–1367 (2001).
15. Xue, Y. & Bogdan, P. Reliable multi-fractal characterization of weighted complex networks: algorithms and implications. *Sci Rep-UK* **7**(1), 7487 (2017).
16. Li, D., Kosmidis, K., Bunde, A. & Havlin, S. Dimension of spatially embedded networks. *Nat Phys* **7**(6), 481–484 (2011).
17. Song, C., Havlin, S. & Makse, H. A. Self-similarity of complex networks. *Nature* **433**(7024), 392 (2005).
18. Zuo, R. & Wang, J. Fractal/multifractal modeling of geochemical data: a review. *J Geochem Explor* **164**, 33–41 (2016).
19. Xue, Y., Pan, W., Lu, W. Z. & He, H. D. Multifractal nature of particulate matters (PMs) in Hong Kong urban air. *Sci Total Environ* **532**(2), 744 (2015).
20. Morató, M. C., Castellanos, M. T., Bird, N. R. & Tarquis, A. M.. Multifractal analysis in soil properties: spatial signal versus mass distribution. *Geoderma.* 54–65 (2017).
21. Sun, C., Liu, G. & Xue, S. Natural succession of grassland on the loess plateau of China affects multifractal characteristics of soil particle-size distribution and soil nutrients. *Eco Res* **31**(6), 1–12 (2016).
22. Bai, Y. & Wang, Y. Monofractal and multifractal analysis on soil particle distribution in hilly and gully areas of the Loess Plateau. *Chin Soc Agr Mac.* **43**(5), 137–140 (2012).
23. Montero, E. Rényi dimensions analysis of soil particle-size distributions. *Eco Model.* **182**(3), 305–315 (2005).
24. Wang, D., Fu, B. J., Chen, L. D., Zhao, W. W. & Wang, Y. F. Fractal analysis on soil particle size distributions under different land-use types: A case study in the loess hilly areas of the Loess Plateau, China. *Acta Ecol Sin.* **27**(7), 3081–3089 (2007).
25. Wang, D. *et al*. Multifractal analysis of land use pattern in space and time: A case study in the Loess Plateau of China. *Ecol Complex.* **7**(4), 487–493 (2010).
26. Hu, Y. F. & Liu, J. Y. Fractal dimension of soil particle size distribution under different land use/land coverage. *Acta Ped Sin.* **42**(2), 336–339 (2005).
27. Wei, X., Li, X. & Wei, N. Fractal features of soil particle size distribution in layered sediments behind two check dams: implications for the Loess Plateau, China. *Geomorphology.* **266**, 133–145 (2016).
28. Kowalenko, C. G. & Babuin, D. Inherent factors limiting the use of laser diffraction for determining particle size distributions of soil and related samples. *Geoderma.* **s193–194**(2), 22–28 (2013).
29. Franzluebbers, A. J. Soil organic matter stratification ratio as an indicator of soil quality. *Soil Till Res.* **66**(2), 95–106 (2002).
30. Herrick, J. E. & Wander, M. M. Soil Processes and the Carbon Cycle (pp. 405–425). Boca Raton, CRC Press (1997). Relationships between soil organic carbon and soil quality in cropped and rangeland soils: the importance of distribution, composition, and soil biological activity. Lal R., Kimble J.M., Follett R.F., Stewart B.A.
31. Kern, J. S., Turner, D. P. & Dodson, R. F. Spatial patterns in soil organic carbon pool size in the Northwestern United States. *Soil Pro Car Cycle* **44** (1997).
32. Jia, X. H. & Xin-Rong, L. I. Soil organic carbon and nitrogen dynamics during the re-vegetation process in the arid desert region. *J. Plant Ecol.* **31**(1), 66–74 (2007).
33. Huang, B. *et al*. Temporal and spatial variability of soil organic matter and total nitrogen in an agricultural ecosystem as affected by farming practices. *Geoderma.* **139**(3), 336–345 (2007).
34. Weng, B. Q., Zheng, X. Z., Ding, H. & Wang, H. P. Effects of vegetation restoration on soil carbon and nitrogen cycles: A review. *J. Appl Ecol.* **24**(24), 3610–3616 (2013).
35. Putten, W. H. V. D. & Wardle, D. A. Plant–soil feedbacks: the past, the present and future challenges. *J. Ecol.* **101**(2), 265–276 (2013).
36. Gao, P., Niu, X., Lv, S. Q. & Zhang, G. C. Fractal characterization of soil particle-size distribution under different land-use patterns in the Yellow River Delta wetland in China. *J Soil Sediment.* **14**(6), 1116–1122 (2014).
37. Fullen, M. A., Booth, C. A. & Brandsma, R. T. Long-term effects of grass ley set-aside on erosion rates and soil organic matter on sandy soils in east Shropshire, UK. *Soil Till Res.* **89**(1), 122–128 (2006).
38. Mantovani, D., Veste, M., Boldt-Burisch, K., Fritsch, S. & Freese, D. Black locust (*Robinia pseudoacacia L.*) root growth response to different irrigation regimes. Meeting of the Ecological Society of Germany, Austria and Switzerland (2013).

39. Hu, X. N. *et al*. Relationship between fine root growth of *Robinia pseudoacacia* plantation and the soil moisture in the Loess Plateau. *Sci Sil Sin*. **46**(12), 30–35 (2010).
40. Qiu, L., Zhang, X., Cheng, J. & Yin, X. Effects of black locust (*Robinia pseudoacacia*) on soil properties in the loessial gully region of the Loess Plateau, China. *Plant Soil* **332**(1), 207–217 (2010).
41. Zhang, C., Liu, G. B., Xue, S., Song, Z. L. & Fan, L. X. Evolution of soil enzyme activities of *Robinia pseudoacacia* plantation at different ages in loess hilly region. *Sci Sil Sin*. **46**(12), 23–29 (2010).
42. Rice, S. K., Westerman, B. & Federici, R. Impacts of the exotic, nitrogen-fixing black locust (*Robinia pseudoacacia*) on nitrogen-cycling in a pine–oak ecosystem. *Plant Ecol*. **174**(1), 97–107 (2004).
43. Uva, R. H., Neal, J. C. & DiTomaso, J. M. Weeds of the Northeast. *Comstock Pub*. Associates (1997).
44. Cal-IPC. California Invasive Plant Inventory. California Invasive Plant Council. Rep. Cal-IPC Publication 2006–02 (2006).
45. Rogerson, C. T. Fungi on plants and plant products in the United States. By David F. Farr; Gerald F. Bills; George P. Chamuris; Amy Y. Rossman. *Mycologia* **42**(3), 243–246 (1990).
46. Zhang, C. H. *et al*. Invasion of *Robinia pseudoacacia* and impacts on native vegetation. *J. Beijing Fore Uni*. **30**(3), 18–23 (2008).
47. Wang, X. C. & Wang, Y. L. Study on the succession of locust forest farm of Yaoxiang. *J. Henan Fore Sci Tec*. **3**, 22–24 (1996).
48. Jung, S. C. *et al*. Reproduction of a *Robinia pseudoacacia*, population in a coastal *Pinus thunbergii*, windbreak along the kujukurihama coast, Japan. *J. Forest Res* **14**(2), 101–110 (2009).
49. Wang, C. C. The pattern, process and mechanism of *Robinia pseudoacacia* sprouting dispersion using SSR in Taishan scenic area. Doctoral dissertation, Shandong Aagricultural University (2016).
50. Greenacre, M. J. Correspondence analysis in practice. *Bms Bull Soc Met*. **65**(41), 50–50 (1993).
51. Giraudel, J. L. & Lek, S. A comparison of self-organizing map algorithm and some conventional statistical methods for ecological community ordination. *Ecol Model*. **146**(1–3), 329–339 (2001).
52. Gui, D. W. *et al*. Ordination as a tool to characterize soil particle size distribution, applied to an elevation gradient at the north slope of the middle kunlun mountains. *Geoderma*. **158**(3), 352–358 (2010).
53. Rejmánek, M., Richardson, D. M. & Pyšek, P. Plant invasions and invasibility of plant communities. *Veg Ecol, Second Edition*, 387–424 (2013).
54. Taguas, F. J., Martın, M. A. & Perfect, E. Simulation and testing of self-similar structures for soil particle-size distributions using iterated function systems. *Geoderma*. **88**(3), 191–203 (1999).
55. Martín, M. A. & Taguas, F. J. Fractal modelling, characterization and simulation of particle-size distributions in soil. *Proc. R. Soc. Lond. A* **454**, 1457–1468 (1998).
56. Telesca, L. & Lapenna, V. Measuring multifractality in seismic sequences. *Tectonophysics* **423**(1), 115–123 (2006).
57. Grant, K. Fundamentals of soil physics. *Engineering Geology* **19**(1), 70–70 (1982).
58. Shi, Z. F., Wang, L. & Wang, J. G. Volume fractal characteristics and significance of soil particles in the Shenmu colliery in north Shanxi Province. *Arid Zone Res*. **28**(3), 394–400 (2011).
59. Liu, Y. Y., Gong, Y. M., Wang, X. & Hu, Y. K. Volume fractal dimension of soil particles and relationships with soil physical-chemical properties and plant species diversity in an alpine grassland under different disturbance degrees. *J Arid Land*. **5**(4), 480–487 (2013).
60. Song, Z., Zhang, C., Liu, G., Qu, D. & Xue, S. Fractal feature of particle-size distribution in the rhizospheres and bulk soils during natural recovery on the Loess Plateau, China. *PloS One*. **10**(9), e0138057 (2015).
61. Su, Y. Z., Zhao, H. L., Zhao, W. Z. & Zhang, T. H. Fractal features of soil particle size distribution and the implication for indicating desertification. *Geoderma*. **122**(1), 43–49 (2004).
62. Pazferreiro, J., Vidal Vázquez, E. & Miranda, J. G. V. Assessing soil particle-size distribution on experimental plots with similar texture under different management systems using multifractal parameters. *Geoderma*. **160**(1), 47–56 (2010).
63. Sperry, J. S. & Hacke, U. G. Desert shrub water relations with respect to soil characteristics and plant functional type. *Funct Ecol*. **16**(3), 367–378 (2002).
64. Raich, J. W. *et al*. Potential net primary productivity in South America: application of a global model. *Ecol Appl*. **1**(4), 399–429 (1991).
65. Ren, X. *et al*. Fractal dimension characteristics of soil particles in oasis desert ecotone in southern edge of Junggar Basin. *J Des Res*. **29**(2), 298–304 (2009).
66. Lobe, I., Amelung, W. & Preez, C. C. D. Losses of carbon and nitrogen with prolonged arable cropping from sandy soils of the South African Highveld. *Eur J Soil Sci*. **52**(1), 93–101 (2001).
67. Wang, H. *et al*. Soil microbial community composition rather than litter quality is linked with soil organic carbon chemical composition in plantations in subtropical China. *J. Soil Sed*. **15**(5), 1094–1103 (2015).
68. Fang, X., Yu, D., Zhou, W., Zhou, L. & Dai, L. The effects of forest type on soil microbial activity in Changbai Mountain, Northeast China. *Ann Forest Sci*. **73**(2), 473–482 (2016).
69. Jackson, R. B., Manwaring, J. H. & Caldwell, M. M. Rapid physiological adjustment of roots to localized soil enrichment. *Nature*. **344**(6261), 58 (1990).
70. Chapin, F. S. & Walker, L. R. Mechanisms of primary succession following deglaciation at glacierbay, Alaska. *Ecol Monogr*. **64**(2), 149–175 (1994).
71. Rubio, A. & Escudero, A. Small-scale spatial soil-plant relationship in semi-arid gypsum environments. *Plant Soil*. **220**(1), 139–150 (2000).
72. Reubens, B., Poesen, J., Danjon, F., Geudens, G. & Muys, B. The role of fine and coarse roots in shallow slope stability and soil erosion control with a focus on root system architecture: a review. *Trees* **21**(4), 385–402 (2007).
73. Zhu, B., Li, Z., Li, P., Liu, G. & Xue, S. Soil erodibility, microbial biomass, and physical–chemical property changes during long-term natural vegetation restoration: a case study in the Loess Plateau, China. *Ecol Res*. **25**(3), 531–541 (2010).
74. Sun, C., Xue, S., Chai, Z., Zhang, C. & Liu, G. Effects of land-use types on the vertical distribution of fractions of oxidizable organic carbon on the Loess Plateau, China. *J. Arid Land*. **8**(2), 221–231 (2016a).
75. Guo, C. *et al*. Simon J. Preferential use of root litter compared to leaf litter by beech seedlings and soil microorganisms. *Plant Soil*. **368**(1), 519–534 (2013).
76. Bittelli, M., Campbell, G. S. & Flury, M. Characterization of particle-size distribution in soils with a fragmentation model. *Soil Sci Soc Am J*. **63**(4), 782–788 (1999).
77. Gray, L. C. & Morant, P. Reconciling indigenous knowledge with scientific assessment of soil fertility changes in southwestern Burkina Faso. *Geoderma*. **111**, 425–437 (2003).
78. Martínez, F. S. J. *et al*. Multifractal analysis of discretized X-ray CT images for the characterization of soil macropore structures. *Geoderma* **156**(1), 32–42 (2010).
79. Miranda, J. G. V., Montero, E., Alves, M. C., González, A. P. & Vázquez, E. V. Multifractal characterization of saprolite particle-size distributions after topsoil removal. *Geoderma* **134**(3), 373–385 (2006).
80. Chen, C. C., Lee, Y. T. & Hasumi, T. Transition on the relationship between fractal dimension and Hurst exponent in the long-range connective sandpile models. *Phys Lett A*. **375**, 324–328 (2011).
81. Wang, D., Fu, B. J., Zhao, W. W., Hu, H. F. & Wang, Y. F. Multifractal characteristics of soil particle size distribution under different land-use types on the Loess Plateau, China. *Catena*. **72**, 29–36 (2008).

82. Yu, J. *et al*. Fractal features of soil particle size distribution in newly formed wetlands in the Yellow River Delta. *Sci Rep* **5**, 10540 (2015).
83. Sun, C., Liu, G. & Xue, S. Natural succession of grassland on the Loess Plateau of China affects multifractal characteristics of soil particle-size distribution and soil nutrients. *Ecol Res.* **31**(6), 1–12 (2016b).
84. Tognetti, P. M. & Chaneton, E. J. Community disassembly and invasion of remnant native grasslands under fluctuating resource supply. *J. Appl Ecol.* **52**(1), 119–128 (2015).
85. Lonsdale, W. M. Global patterns of plant invasions and the concept of invasibility. *Ecology.* **80**(5), 1522–1536 (1999).
86. Campbell, C., Yang, S., Albert, R. & Shea, K. Plant-pollinator community network response to species invasion depends on both invader and community characteristics. *Oikos* **124**(4), 406–413 (2015).
87. Zheng, J. & Ma, K. Research advances in the relationships between biodiversity and invasiveness within forest communities. *Chin J Appl Ecol.* **17**(7), 1338–1343 (2006).
88. Zalba, S. M., Sonaglioni, M. I., Compagnoni, C. A. & Belenguer, C. J. Using a habitat model to assess the risk of invasion by an exotic plant. *Biol Conserv.* **93**(2), 203–208 (2000).
89. Frappier, B. & Eckert, R. T. Utilizing the USDA PLANTS database to predict exotic woody plant invasiveness in newHampshire. *Forest Ecol Man.* **185**(1–2), 207–215 (2003).
90. Thuiller, W. *et al*. Niche-based modelling as a tool for predicting the risk of alien plant invasions at a global scale. *Global Change Biol.* **11**(12), 2234–2250 (2005).
91. Hirzel, A. H., Hausser, J., Chessel, D. & Perrin, N. Ecological-niche factor analysis: how to compute habitat-suitability maps without absence data? *Ecology* **83**(7), 2027–2036 (2008).
92. Rubin, E. S., Stermer, C. J., Boyce, W. M. & Torres, S. G. Assessment of predictive habitat models for bighorn sheep in California's Peninsular ranges. *J. Wildlife Manage.* **73**(6), 859–869 (2015).
93. Davis, M. A., Grime, J. P. & Thompson, K. Fluctuating resources in forest communities: a general theory of invasibility. *J. Ecol.* **88**(3), 528–536 (2000).
94. Ehrenfeld, J. G. & Scott, N. Invasive species and the soil: effects on organisms and ecosystem processes. *Eco Appl.* **11**(5), 1259–1260 (2001).
95. Levine, J. M. *et al*. Mechanisms underlying the impacts of exotic plant invasions. *P Roy Soc Lond B Bio* **270**(1517), 775 (2003).
96. Zheng, J. M., Jun-Qing, L. I. & Sun, Q. X. Review of ecological prediction and risk analysis on woody plant invasion. *Acta Ecol Sin.* **28**(11), 5549–5560 (2008).
97. Blackburn, T. M. & Duncan, R. P. Determinants of establishment success in introduced birds. *Nature.* **414**(414), 195–197 (2001).
98. Rényi, A. Probability Theory. **53**(1), 5–26 (1970).
99. Hentschel, H. G. E. & Procaccia, I. The infinite number of generalized dimensions of fractals and strange attractors. *Physica D* **8**(3), 435–444 (1983).
100. Chhabra, A. & Jensen, R. V. Direct determination of the f (α) singularity spectrum. *Phys Rev Lett.* **62**(12), 1327 (1989).
101. Kravchenko, A. N., Boast, C. W. & Bullock, D. G. Multifractal analysis of soil spatial variability. *Agron J.* **91**(6), 1033–1041 (1999).
102. Kantelhardt, J. W. *et al*. Multifractal Detrended Fluctuation Analysis of nonstationary time series. *Physica A* **316**(1), 87–114 (2002).
103. Salat, H., Murcio, R. & Arcaute, E. Multifractal methodology. *Physica A* **473**, 467–487 (2017).
104. Chamoli, A. & Yadav, R. B. S. Multifractality in seismic sequences of NW Himalaya. *Nat Hazards* **77**(1), 19–32 (2015).

Acknowledgements

The authors are grateful for the financial support provided by the National Special Fund for Industry Public Welfare (Project No. 201504406) and the National Natural Science Foundation of China (Project No. 31570705). Additionally, this paper was supported by the CFERN & GENE Award Funds on Ecological Paper. The authors are also grateful for the comments of the anonymous reviewers.

Author Contributions

Kun Li and Chuanrong Li designed the study. Huanxiang Yang, Xu Han, Lingyu Xue, Weixing Shen, Huiling Guo and Yikun Zhang collected the soil samples. Yang Lv, Jinhua Li and Zhanyong Fu performed the experiments. Kun Li analyzed the data and wrote the manuscript. All the authors reviewed and approved the final manuscript.

Additional Information

Competing Interests: The authors declare no competing interests.

Publisher's note: Springer Nature remains neutral with regard to jurisdictional claims in published maps and institutional affiliations.